Acta Biochimica Polonica

Vol. 46 No. 3/1999

651–663

QUARTERLY

NMR measurements of proton exchange between solvent and peptides and proteins*°

Jacek Wójcik, Katarzyna Ruszczyńska, Igor Zhukov and Andrzej Ejchart✉

Institute of Biochemistry and Biophysics, Polish Academy of Sciences, A. Pawińskiego 5A, 02-106 Warszawa, Poland

Received: 07 July, 1999

Key words: proton exchange, NMR methods, magnetization transfer

Scope and limitations of the NMR based methods, equilibration and magnetization transfer, for measuring proton exchange rates of amide protons in peptides and proteins with water protons are discussed. Equilibration is applied to very slow processes detected by hydrogen-deuterium exchange after a solute is dissolved in D_2O. Magnetization transfer allows to study moderately rapid processes in H_2O. A number of precautions should be undertaken in order to avoid systemic errors inherent in the magnetization transfer method.

Proton exchange with solvent water protons is a powerful technique for studying structure and dynamics of peptides and proteins [1, 2]. Nuclear magnetic resonance (NMR) spectroscopy is one of the most suitable tools to perform such studies. Observation of labile amide protons carried out over a range of pH values allows to determine rate constants, k, for acid- and base-catalyzed exchange. The exchange rates provide information about such features of molecules as solvent accessibility, complexation sites, and stability of hydrogen-bonded secondary and tertiary structures [1, 3, 4].

The rates at which amide protons in biomolecules, H_N, are exchanged with water

*Presented at the symposium "Conformation of peptides, proteins and nucleic acids" held in Rynia, Poland, on 26–29 May, 1999.

°This work was financially supported by grant 6 P04A 009 16 from the State Committee for Scientific Research (KBN).

✉Correspondence to: Andrzej Ejchart, phone/fax: (48 22) 658 4683, e-mail: aejchart@ibb.waw.pl

Abbreviations: CMTI-I, *Cucurbita maxima* trypsin inhibitor type I; NMR, nuclear magnetic resonance; NOE, nuclear Overhauser effect; PFG, pulsed field gradient; EXSY, exchange spectroscopy; HMQC, heteronuclear multiple quantum coherence; HSQC, heteronuclear single quantum coherence; DANTE, delays alternating with nutation for tailored excitation; WANTED, water selective DANTE using gradients; WATERGATE, water suppression by gradient tailored excitation; MEXICO, measurement of exchange rates of isotopically labeled compounds.

vary over many orders of magnitude [2]. Availability of the exchange process parameters to NMR measurements depends on the localization of its rate in the NMR timescale. The latter can be visualized taking as an example a simple two-site exchange between two equally populated sites. If the exchange rate is substantially lower than the frequency difference between resonances of individual sites ($k/\Delta f << 1$), two sharp signals appear and the system is in the slow exchange regime. When the exchange rate increases, successive broadening and merging of the signals occurs and at $k/\Delta f = \pi/2^{1/2} \approx 2.22$ they merge. This situation is referred to as coalescence. A further increase of the exchange rate results in signal narrowing as the fast exchange regime is approached ($k/\Delta f >> 1$). The intermediate rates of exchange are placed between slow and fast exchange regions (Fig. 1). Therefore, the frequency difference between exchanging resonances determines the NMR timescale [5, 6].

Since numerous protons in peptides and proteins exchange with solvent molecules at the same time, the exchange process(es) can be studied only at the rates when individual resonances of exchangeable solute protons are observed i.e. below the values at which coalescence does appear. The lineshape analysis of exchange-broadened signals, a method widely used in the chemical exchange studies of small organic molecules, cannot be successfully used for studying exchange processes because numerous overlapping H_N signals preclude accurate determination of exchange rates. Therefore, only two, among many, NMR methods are applicable to such studies: equilibration and magnetization transfer.

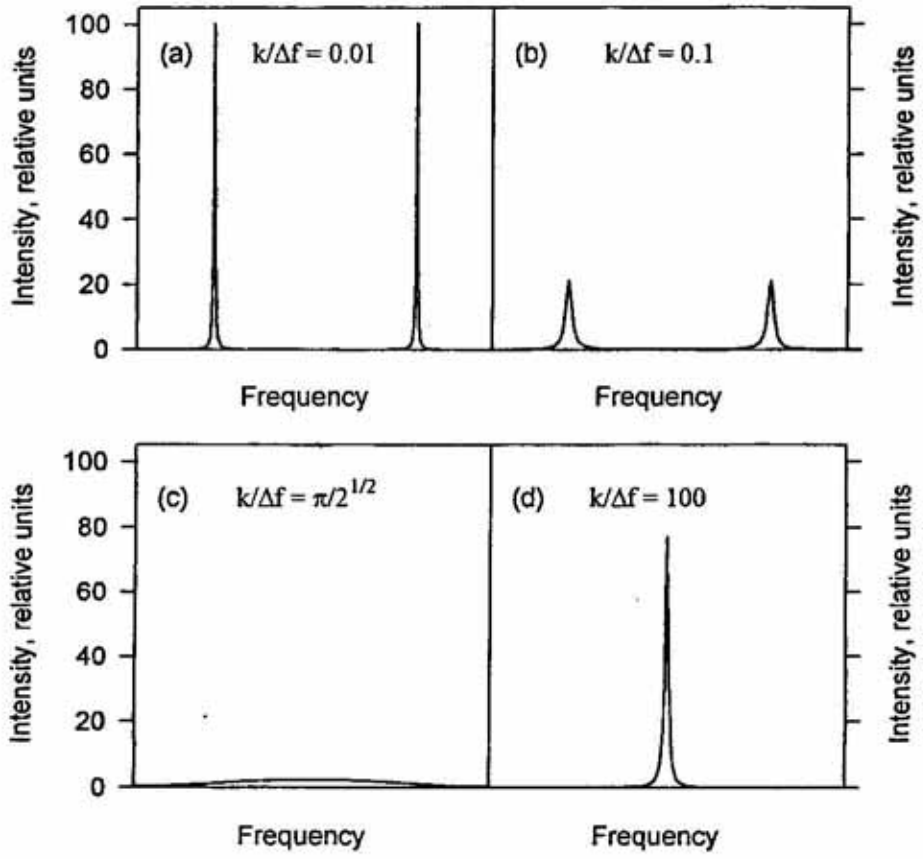

Figure 1. Calculated NMR lineshapes for equally populated two-site exchange at the slow exchange regime (a), at the intermediate exchange region below the coalescence point (b), at the coalescence point (c) and close to the fast exchange regime (d).

EQUILIBRATION METHOD

Equilibration is applicable to very slow processes and it relies on the determination of amide exchange rates by hydrogen-deuterium exchange using suitable NMR spectra acquired consecutively to detect the progress of deuterium substitution after the protein or peptide has been dissolved in D_2O [7]. Because the H_N signals in one-dimensional ^1H NMR spectra of proteins, except those for small peptides, tend to overlap, two-dimensional techniques, both homonuclear [8] and heteronuclear [9], are usually used to increase spectral dispersion. The rate of exchange at a given amide site is obtained from a simple exponential fit of the H_N signal intensities/integrals as a function of exchange time. Assuming that the first spectrum can be collected 5 min after a protein was dissolved and that no more than 50% substitution took place in that period, the exchange rates slower than 0.002 s^{-1} (0.12 min^{-1}) are accessible to this method. Since a great number of amide protons in proteins exhibit lifetimes of hours or days, equilibration, as a method which is simple from the technical standpoint, has been often used in studies of proton exchange [10–13].

MAGNETIZATION TRANSFER METHOD

The magnetization transfer method allows to study moderately rapid proton exchange below the coalescence point. A number of techniques and many modifications have been proposed since the first paper on the subject by Forsén & Hoffman [14] was published. Since for such a study H_2O, rather than D_2O, must be used as a solvent, it is necessary to observe the solute signals in the presence of the solvent peak which is about 10^5 times more intense. This dynamic range problem, inherent to the majority of the NMR measurements of biological molecules [15], is particularly severe in the case of exchange studies when the magnetization of solvent nuclei should be handled with a special care. A convenient and simple method for overcoming the problem is selective saturation of the solvent resonance. Inversion should be avoided as it leads to the ra-

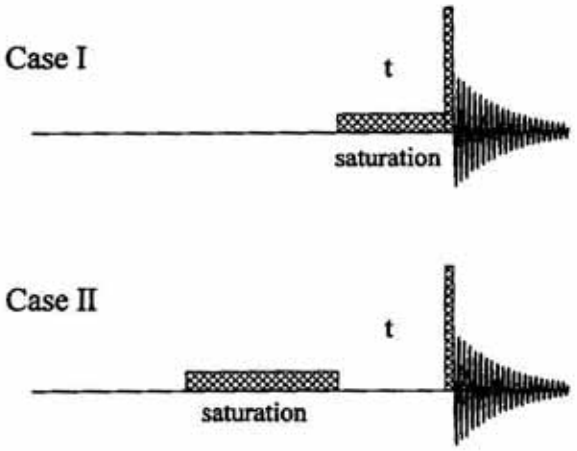

Figure 2. Two different types of magnetization transfer pulse sequence proposed by Forsén & Hoffman [14].

In Case I the decay of H_N signal upon progressive selective saturation of solvent resonance is a single-exponential function of the saturation time, t, (Eqn. 1). Solvent saturation has to occur instantaneously at time $t = 0$. In Case II the recovery of H_N signal upon removal of the solvent resonance saturation is observed as a bi-exponential function of the recovery time, t, (Eqn. 2). Solvent saturation should be long enough to establish a steady-state condition. Narrow vertical bars represent the read sequence. In the simplest case it can be a 90° pulse but usually more sophisticated sequences allowing to avoid solvent resonance excitation and/or improving spectral dispersion are used.

diation damping [16], which accelerates the return of the water magnetization to equilibrium. The problem can be resolved by the use of pulse sequences incorporating field gradients [17].

Standard magnetization transfer pulse sequences adapted from Forsén & Hoffman [14] to pulsed spectrometers are presented in Fig. 2. As follows from the solution of McConnell equations [18] under the assumption of great excess of solvent, H_N signal intensities/integrals, I, depend on the saturation or recovery time, t, according to the equations:

Case I

$$I(t) = I_0\{[k/(k+\rho)] \cdot \exp[-(k+\rho)t] + \rho/(k+\rho)\} \quad (1)$$

Case II

$$I(t) = I_0\{1 + [k/(\rho_w - \rho - k)] \cdot \exp[-\rho_w t] - [k\rho_w/(k+\rho) \cdot (\rho_w - \rho - k)] \cdot \exp[-(k+\rho)t]\} \quad (2)$$

In addition to the exchange rate, k, two additional parameters appear in Eqns. 1 and 2, longitudinal relaxation rates of solute H_N, ρ, and water protons, ρ_w. The latter should be determined in a separate experiment. I_0 represents the equilibrium value of I [14].

Since limits of intensity changes in both cases are I_0 and $I_0\rho/(k+\rho)$, the k/ρ ratio determines magnitudes of exchange rates accessible to this method. In order to observe well measurable intensity changes indispensable for data reduction of good quality, the condition $\rho/(k+\rho) < 0.9$ should be fulfilled. Therefore, if the condition $k/\rho > 0.1$ does not hold, accuracy of the exchange rate determination deteriorates as shown in Fig. 3 [19]. Longitudinal relaxation rates of the H_N protons strongly depend on the molecular mass of solute, temperature and the magnetic field strength of the NMR spectrometer; most often these rates are in the range $0.5\ s^{-1} < \rho < 10\ s^{-1}$ [20–22]. On the other hand, the upper limit of the exchange rate should be well below the exchange rate of coalescence. Calculated NMR lineshapes of the H_N protons exchanging with solvent protons in typical experimental conditions are shown in Fig. 4. Exchange broadening, which brings about a 5-fold decrease of intensity, seems to be a tolerable limit from the standpoint of signal to noise ratio, thus giving $k < 20\ s^{-1}$.

Summing up, the magnetization transfer method allows to determine exchange rates over the range [0.05 s^{-1}, 20 s^{-1}]. It should be pointed out that there is a gap between the upper limit of exchange rates available to the equilibration method (0.002 s^{-1}) and the lower limit of exchange rates available to the magnetization transfer method. Nevertheless, the magnetization transfer method has been widely used for determination of the exchange rates of amide protons in peptides and proteins with water [11, 13, 23–25].

PROBLEMS SPECIFIC TO THE MAGNETIZATION TRANSFER METHOD

There are several types of problems inherent in the determination of H_N exchange rates with solvent by the magnetization transfer method: (1) efficient generation of the nonequilibrium initial state, (2) spectral dispersion allowing to observe individual, non-overlapping signals, (3) read pulse/sequence avoiding excitation of solvent resonance, (4) reliable and accurate data reduction, (5) spurious pathways of the magnetization transfer disturbing the observed intensities/integrals of H_N resonances.

Ad 1. As mentioned above, selective saturation of water magnetization, rather than its inversion, has been widely used in order to avoid the radiation damping. Selective satura-

tion, however, used progressively (Case I) does not suppress completely the large water signal at short saturation times. Moreover, short saturation times lead to the enhancement of radiation damping. In consequence, the apparent k and ρ values are underestimated (cf. Fig. 5). An elegant approach overcoming this deficiency was proposed by Adams & Lerner [26]. A weak, variable-length spin-lock pulse sandwiched between two selective 90° pulses is used rather than progressive selective saturation.

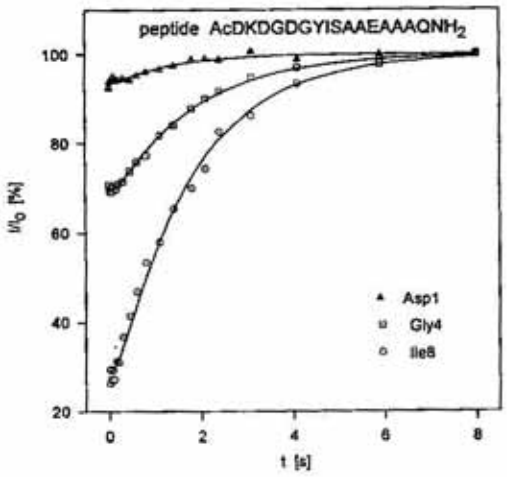

Figure 3. Experimental data and least-squares fits for three selected residues in the 16-residue peptide analogous to the 3rd calcium binding loop of calmodulin saturated with La^{3+} ions (Case II, Eqn. 2).

The k/ρ ratio influences the accuracy of the parameter determination. For Asp1 (k/ρ = 0.07) relative standard errors of exchange parameters are large: k = 0.05 s^{-1} (17%) and ρ = 0.76 (20%). For two other residues relative standard errors are much smaller: Gly4 (k/ρ = 0.45), k = 0.18 s^{-1} (4%), ρ = 0.40 (4%) and Ile8 (k/ρ = 2.47), k = 0.43 s^{-1} (6%), ρ = 0.17 (6%). Water relaxation rate, ρ_w = 4.9 s^{-1} [19].

New possibilities have become available for the NMR spectrometers equipped with pulse field gradient (PFG) hardware. Many sequences with PFGs have been invented recently [17]. One of them, the WANTED sequence [27], allows to excite the water resonance with the selective 90° or 180° DANTE pulse [28] applying bipolar gradient pulses during DANTE delays. Such pulses quench efficiently the radiation damping.

Ad 2. Well separated H_N signals can be solely observed in small peptides. Partial overlapping of H_N signals usually occurs in peptides comprising twelve or more amino-acid residues as seen in Fig. 6. Resorting to two-dimensional EXSY spectra [29] does not help because all correlation peaks between H_N and water protons appear at the position of the chemical shift of water resonance [30]. That is why the peaks of interest display a spectral dispersion similar to that observed in corresponding one-dimensional spectra.

If overlapping H_N protons are scalar coupled with well separated H_α protons, a double-selective spin-lock can be used for an additional magnetization transfer step $H_N \rightarrow H_\alpha$. The intensity of H_α protons is monitored, rather than that of H_N, to study the amide proton exchange rate [22]. However, the best dispersion of H_N signals is obtained in heteronuclear $^1H/^{15}N$ correlation spectra, HMQC [31, 32] and HSQC [33], of ^{15}N-labeled peptides and proteins. $^1H/^{15}N$ HSQC spectrum of the Met8→Leu mutant of *Cucurbita maxima* trypsin inhibitor type I, CMTI-I (M8L), a small 29 amino-acid residue protein clearly demonstrates the possibility of very good separation of amide correlation peaks. This two-dimensional HSQC spectrum contrasted with a corresponding part of one-dimensional ^1H NMR spectrum is shown in Fig. 7. All 27 signals of the backbone amide protons are well separated in the HSQC spectrum, whereas only 7 H_N protons show non-overlapping signals in the one-dimensional ^1H NMR spectrum. Use of the HSQC sequence allowed to determine exchange rates with water and relaxation rates for almost all amide backbone protons in CMTI-I (M8L) protein (cf. Fig. 8).

Ad. 3. Read pulse sequences avoiding excitation of strong solvent resonance, that replace the last pulse in the one-dimensional or multidimensional technique, have been used for a long time in NMR of biological systems [34]. One of the most popular sequences is the

Jump-and-Return one [35], the simplest of the so-called binomial sequences. It comprises two 90° pulses of opposite phase separated by a delay τ. On-resonance water signal ends the Jump-and-Return sequence aligned with $+z$ axis, whereas the excitation maxima occur at $\pm 1/4\tau$ (Fig. 9). If pulse field gradients are available, the WATERGATE sequence can be used [36]. It is a modified PFG spin-echo sequence with 180° refocusing pulse flanked by two selective 90° pulses [17, 37]. The combined effect of these three pulses is a net zero rotation of the water magnetization. Hence, both gradient pulses dephase the transverse water magnetization but refocus the solute one (Fig. 9).

The influence of the read sequence on the determination of exchange rates has been studied on selected H_N backbone protons in the 14-residue peptide, analogous to the 3rd calcium binding loop of calmodulin saturated with La^{3+} ions. Signal intensities were measured as a function of the recovery time (Case II) using the Jump-and-Return and WATERGATE read sequences. The results obtained for three residues of this peptide are given in Table 1. They do not differ within experimental errors. However, the standard errors of parameters calculated for the data acquired with the Jump-and-Return sequence are larger than those acquired using WATERGATE, ow-

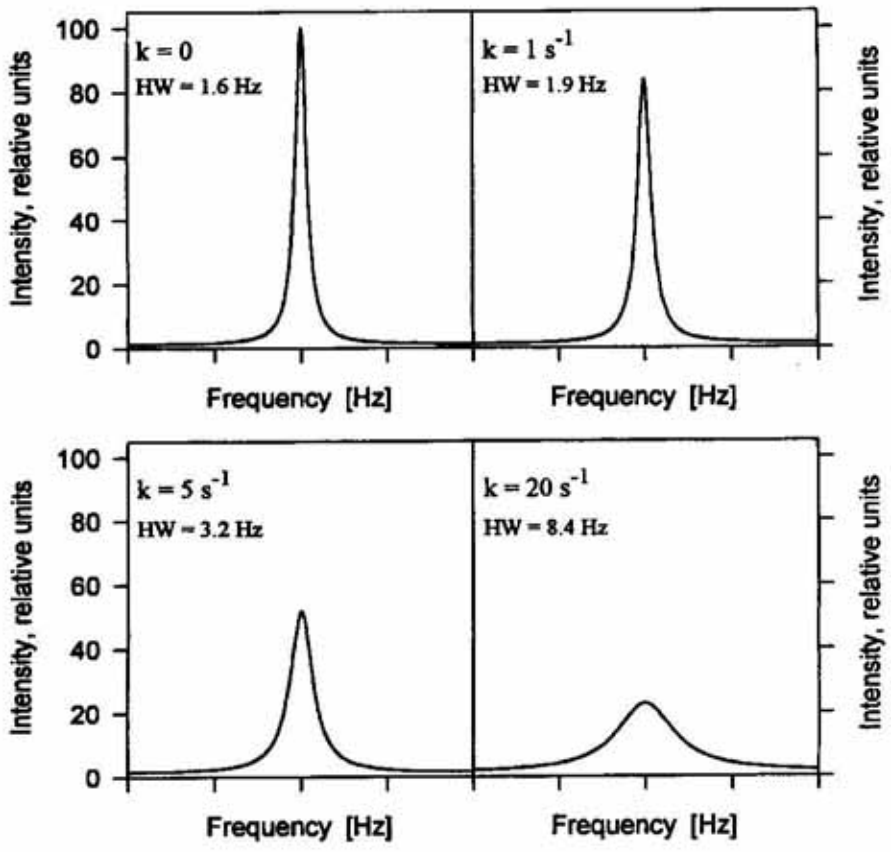

Figure 4. Calculated NMR lineshapes of H_N protons exchanging with water.

It was assumed that solute concentration, c = 1 mM, and transverse relaxation times, $T_2(H_N)$ = 0.2 s, $T_2(H_2O)$ = 0.5 s. Frequency difference, $\Delta f = f(H_N) - f(H_2O)$ = 1500 Hz, corresponds to 3 ppm at 500 MHz, an average chemical shift difference between water and amide proton resonances. Signal broadening resulting in a 5-fold decrease of amplitude (at k = 20 s^{-1}) seems to be the upper limit of the exchange rates studied by the magnetization transfer method. Widths at half-height of the lineshape, HW, are given in the Figure. The distance between tick marks on the abscissa corresponds to 10 Hz.

ing to the strong baseline corruption inherent in the former read sequence.

Ad. 4. Several conditions should be met in order to obtain a reliable exchange rate determination from raw experimental data. Precise determination of the solvent relaxation rate, ρ_w, for the Case II method significantly influences the accuracy of k and ρ values because these three parameters are strongly correlated and multiple local minima can exist. That is why ρ_w has to be determined independently. Including ρ_w into the set of fitted parameters leads to very large parameter inaccuracies. This is the case even if simultaneous fit for parameters of several H_N protons and global ρ_w value is performed despite the increased number of degrees of freedom for a system (cf. Fig. 10 and Table 2).

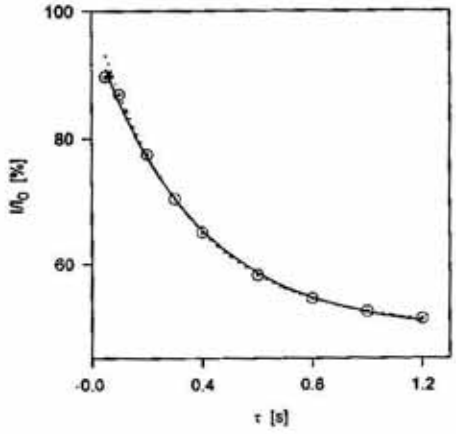

Figure 5. Effect of non-immediate progressive water saturation.

The dotted line represents the H_N signal decay for the ideal progressive saturation experiment (Case I) with immediate water saturation. Open circles correspond to the data obtained in a fictitious non-ideal experiment with water saturation building up with a time constant of 15 ms. Solid line represents the best least-squares fit to those data. The ideal experiment was computed assuming $k = \rho = 1.5\ s^{-1}$. The best fit to the non-ideal data gives: $k = 1.32 \pm 0.08\ s^{-1}$ and $\rho = 1.35 \pm 0.11\ s^{-1}$.

Results of several optimization approaches applied to the experimental data of the H_N signal recovery (Case II) are given in Table 2. If three parameters, k, ρ and ρ_w, are fitted, two minima are found (Table 2, B). Target function values corresponding to these minima are identical within the computer's floating point precision and no preference can be given to any of these solutions; standard errors are unacceptably large. The accuracy is improved for the simultaneous fit of the data obtained for three different H_N protons: Ile8, Ser9, and Ala10 (Table 2, D). In this approach one of the two minima could be excluded but standard errors remain large. Strong correlation among the fitted parameters has been proven by substituting the calculated ρ_w values as constants and, thus, reducing the number of fitted parameters. In this way, a threefold reduction of standard errors has been obtained (Table 2, C). The results obtained using the ρ_w value measured in a separate experiment are given for comparison (Table 2, A).

Ad. 5. As pointed out by Spera *et al.* [20], in proteins occur phenomena which can disturb magnetization transfer caused by the exchange of amide protons with water. All of them are related to cross-relaxation – a mechanism allowing for exchange of magnetization between two dipolar coupled spins [38]. Experimental manifestation of cross-relaxation, the nuclear Overhauser effect (NOE) is a net magnetization change in the intensity/integral of a nuclear spin resonance when the resonance of another dipolar coupled spin is perturbed [39, 40]. In a system of two dipolar coupled, exchanging spins magnetization transfer occurs *via* two independent pathways, chemical exchange with the rate – k and cross-relaxation with the rate – σ [41, 42]. Computational separation of these two contributions to the total magnetization transfer obtained in experiment is difficult, if possible at all. In proteins a spurious magnetization transfer can occur *via*: (a) incidental saturation of H_α protons resonating close to the water signal and NOE transfer to nearby H_N protons, (b) direct (single step) and/or indirect (multistep) NOE transfer between water and H_N, (c) NOE transfer from nearby, labile OH proton which is saturated *via* exchange with

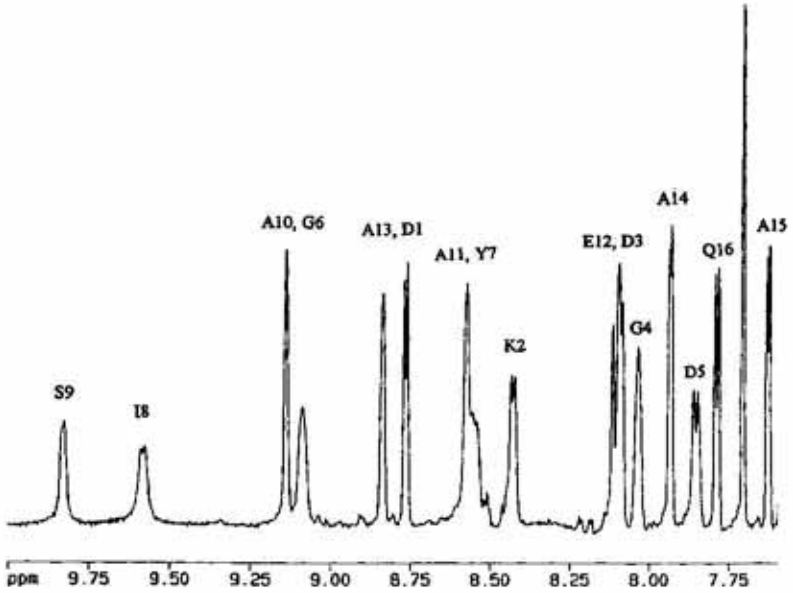

Figure 6. The H_N region of ^1H NMR spectrum of the 16-residue peptide (peptide sequence is given in Fig. 3). Several H_N resonances overlap precluding their quantitative analysis.

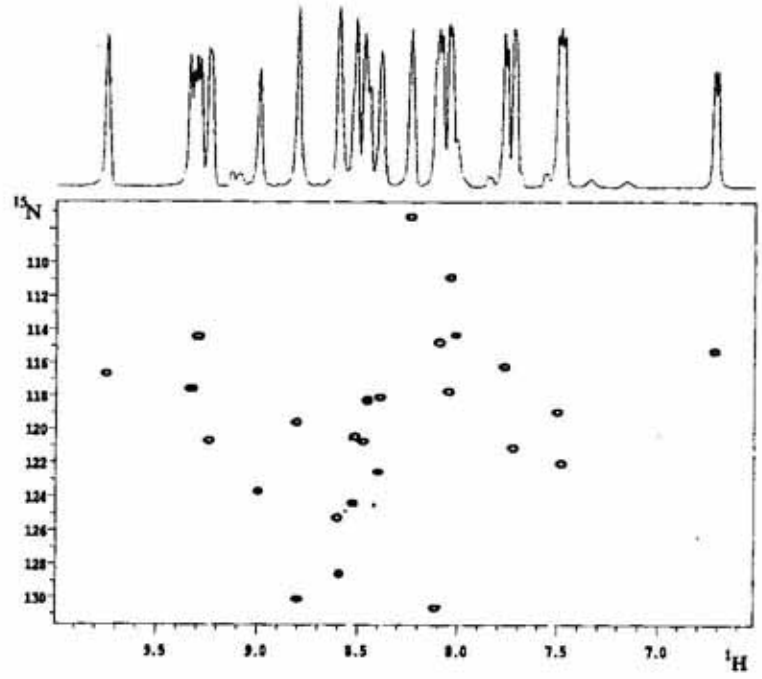

Figure 7. $^1H/^{15}N$ HSQC spectrum of backbone amide groups in the CMTI-I (M8L) protein and the corresponding portion of one-dimensional ^1H NMR spectrum.

Spreading out the signals in ^{15}N dimension removes their overlap in ^1H dimension.

water, an effect often observed in Ser and Thr residues (cf. Fig. 11) [20]. All these effects can be detected and identified, but not eliminated, using NMR methods introduced by Kriwacki *et al.* [43].

Efforts have been made to eliminate cross-relaxation effects in the determination of exchange rates by the magnetization transfer method. Spera *et al.* [20] measured magnetization transfer from water to H_N protons at different pH values and separated an exchange contribution from a cross-relaxation contribution assuming that the latter is independent of the pH value. A different approach, which can be applied to proteins double-labeled with ^{15}N and ^{13}C, has been proposed by Gemmecker *et al.* [44]. Two-dimensional pulse sequence, MEXICO, allows to minimize NOE effects with the carbon-bound protons. This sequence, however, does not suppress cross-relaxation between H_N protons and water or rapidly exchanging OH protons.

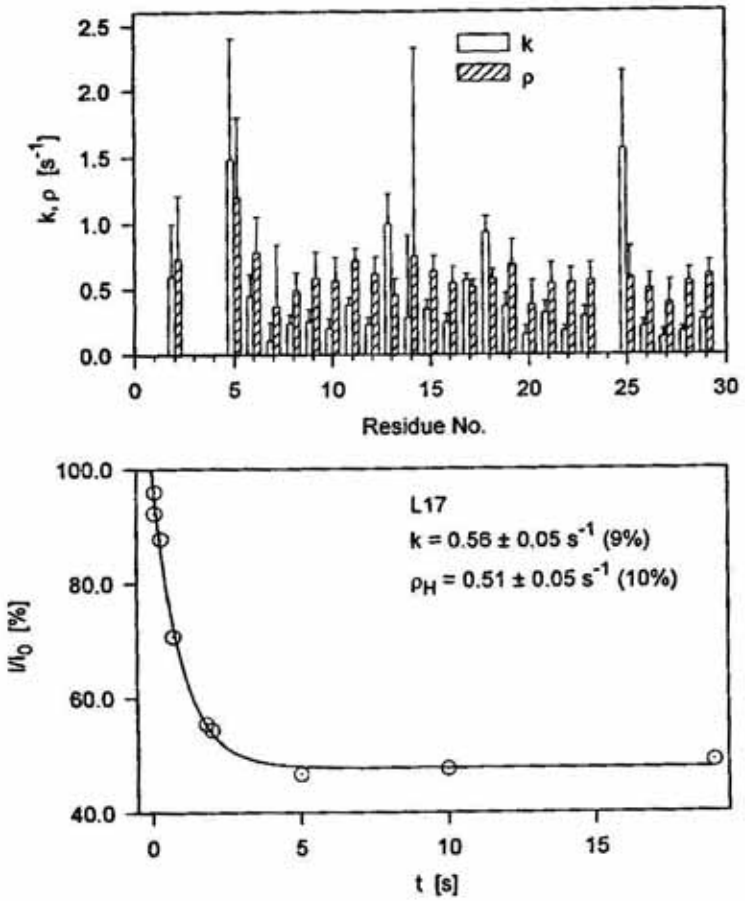

Figure 8. Exchange rates of amide protons with water, k, and their longitudinal relaxation rates, ρ, measured in the CMTI-I (M8L) protein using progressive water saturation (Case I).

Error bars are shown in the Figure. Quality of the fit is presented for the Leu17 residue.

EXPERIMENTAL

The 14-residue peptide analogous to the 3rd calcium binding loop of calmodulin, GDKDGDGYISAAEhS, was obtained as described in an accompanying paper [45]. The peptide was dissolved in H_2O/D_2O (9:1) containing 100 mM NaCl and 20 mM $LaCl_3$. pH was set at 5.7 and the final peptide concentration was 4 mM. NMR measurements were performed on a Varian Unity+ 500 spectrometer at 275 K. Magnetization transfer was performed using the Case II sequence with saturation delay 8 s and 11 different recovery delays: 0.005,

Table 1. Exchange parameters obtained for amide protons of three residues in the peptide GDKDGDGYISAAEhS.

Data were acquired with two read sequences, Jump-and-Return (JR) and WATERGATE (WG), and fitted to Eqn. 2 (Case II). ρ_w, determined in a separate experiment, is equal to $1.10 \pm 0.02\ s^{-1}$. Better accuracy has been obtained for the WATERGATE sequence. Standard errors of parameters are given in parentheses.

Residue	Sequence	k (δk) [s^{-1}]	ρ ($\delta\rho$) [s^{-1}]
Ile8	WG	1.03 (0.10)	0.88 (0.09)
	JR	0.9 (0.3)	1.4 (0.5)
Ser9	WG	0.44 (0.10)	3.1 (0.6)
	JR	0.7 (0.4)	3.6 (1.9)
Ala10	WG	0.51 (0.04)	0.93 (0.09)
	JR	0.49 (0.07)	1.2 (0.2)

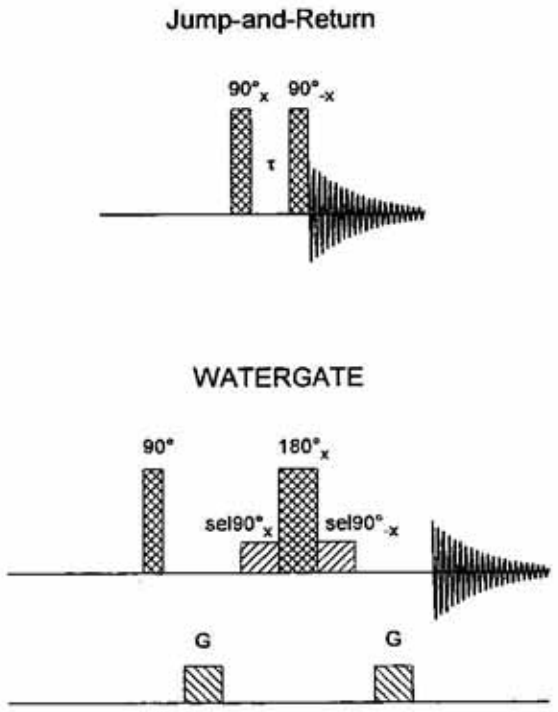

Figure 9. Two read sequences avoiding water excitation: Jump-and-Return and WATERGATE.

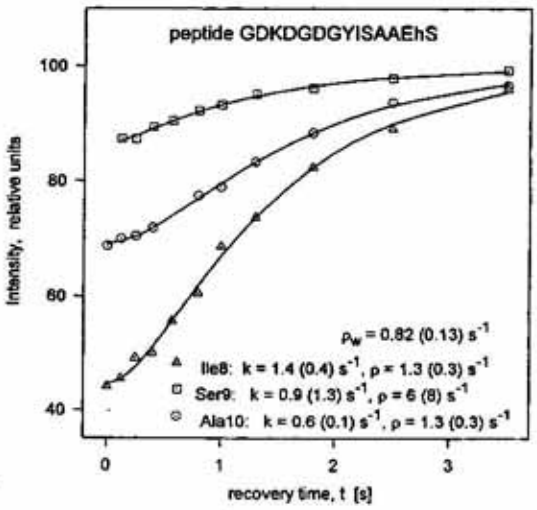

Figure 10. Global least-squares fit performed for the measurement of exchange of H_N protons of three amino-acid residues in the 14-residue peptide analogous to the 3rd calcium binding loop of calmodulin saturated with La^{3+} ions (Case II, Eqn. 2).

k_i and ρ_i for each amino-acid residue and ρ_w common for all H_N (total–7 fitted parameters) were fitted applying weights inversely proportional to relative errors equal to $\delta P_i/P_i$. The best fit curves and calculated parameters are shown in the Figure. Parameters obtained in separate fits for each residue using the ρ_w value measured in an independent experiment are given in Table 1 (WG).

0.12, 0.25, 0.4, 0.57, 0.8, 1, 1.3, 1.8, 2.5, and 3.5 s. Longitudinal water relaxation, ρ_w, was measured using the progressive saturation technique [46] with the same delays as in magnetization transfer measurements.

Synthesis and NMR measurements of the 16-residue peptide analogous to the 3rd calcium binding loop of calmodulin, AcDKDGDGYISAAEAAAQHN$_2$, were described by Ejchart *et al.* [19].

Overexpression, purification and NMR measurements of the Met8→Leu mutant of

Table 2. Results of several fittings of the data obtained for the H_N proton of Ile8 residue in the peptide GDKDGDGYISAAEhS to Eqn. 2 (Case II); read sequence – WATERGATE.

Experimental data and the best fit curve are shown in Fig. 10. The minimum of target function $F = [\sum_i (I_{i,exp} - I_{i,calc})^2/n]^{1/2}$ was searched for in the optimization procedure. Standard errors of parameters are given in parentheses.

	k (δk) [s^{-1}]	ρ ($\delta\rho$) [s^{-1}]	ρ_w ($\delta\rho_w$) [s^{-1}]	F	Comments
A	1.03 (0.10)	0.88 (0.09)	1.10 (0.02)*	0.983	ρ_w-measured
B	0.44 (0.10)	0.36 (0.10)	2.9 (1.1)	0.922	ρ_w-fitted
	1.62 (0.67)	1.30 (0.46)	0.8 (0.2)	0.922	
C	0.44 (0.03)	0.36 (0.03)	2.9	0.922	ρ_w-assumed
	1.62 (0.20)	1.30 (0.15)	0.8	0.922	(taken from B)
D	1.55 (0.39)	1.25 (0.27)	0.82 (0.13)	0.923	ρ_w-global fit

*Participation of $\delta\rho_w$ in δk and $\delta\rho$ was calculated and appropriate corrections were included in the reported values.

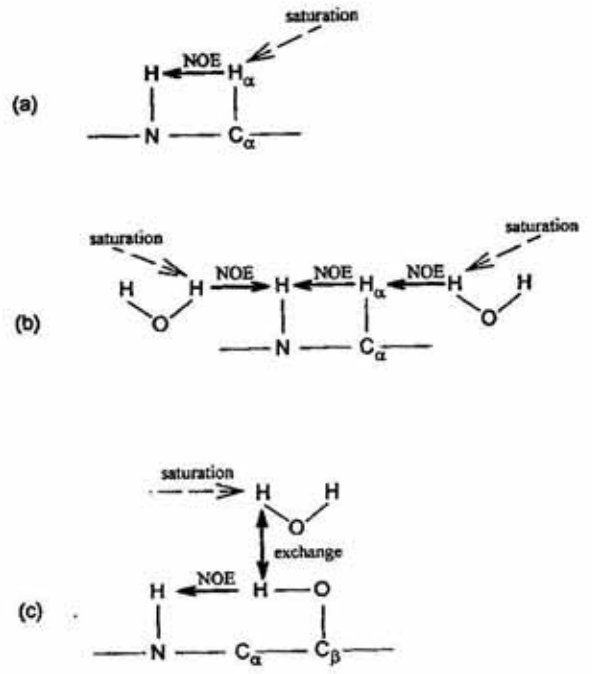

Figure 11. Spurious, cross-relaxation related magnetization transfer pathways disturbing proton exchange measurements by the means of magnetization transfer method.

(a), (b) and (c) refer to the cases discussed in the text.

Cucurbita maxima trypsin inhibitor type I, are described in accompanying paper [47]. Magnetization transfer was performed using the Case I sequence with a relaxation delay 10 s and 9 saturation delays: 0.1, 0.1, 0.3, 0.7, 1.8, 2, 5, 10, and 19 s.

CONCLUSIONS

A study of the exchange rates of amide protons in peptides and proteins with water by means of NMR spectroscopy requires a properly chosen experimental method. The equilibration is the method of choice in the case of very slow exchange, $k < 0.002\ s^{-1}$. The magnetization transfer method allows to determine faster exchange rates over the range [0.05 s^{-1}, 20 s^{-1}]. There are, however, many pitfalls inherent in this method. Therefore, appropriate precautions should be undertaken in order to obtain reliable results.

REFERENCES

1. Englander, S.W. & Englander, J.J. (1978) Hydrogen – tritium exchange. *Methods Enzymol.* **49**, 24–39.
2. Englander, S.W. & Kallenbach, N.R. (1983) Hydrogen exchange and structural dynamics of proteins and nucleic acids. *Q. Rev. Biophys.* **16**, 521–655.
3. Henry, H.D. & Sykes, B.D. (1990) Hydrogen exchange kinetics in a membrane protein determined by ^{15}N NMR spectroscopy: Use of the INEPT experiment to follow individual amides in detergent-solubilized M13 coat protein. *Biochemistry* **29**, 6303–6313.
4. Linse, S., Teleman, O. & Drakenberg, T. (1990) Ca^{2+} binding to calbindin D_{9k} strongly affects backbone dynamics: Measurements of exchange rates of individual amide protons using ^{1}H NMR. *Biochemistry* **29**, 5925–5934.
5. Sandström, J. (1982) *Dynamic NMR Spectroscopy.* Academic Press, London.
6. Lian, L.Y. & Roberts, G.C.K. (1993) *NMR of Macromolecules. A Practical Approach* (Roberts, G.C.K., ed.) pp. 153–182, Oxford University Press, Oxford.
7. Patel, D.J. & Canuel, L.L. (1976) Nuclear magnetic resonance studies of slowly exchanging peptide protons in cytochrome *c* in aqueous solution. *Proc. Natl. Acad. Sci. U.S.A.* **73**, 1398–1402.
8. Wagner, G. & Wüthrich, K. (1982) Amide proton exchange and surface conformation of the basic pancreatic trypsin inhibitor in solution. *J. Mol. Biol.* **160**, 343–361.
9. Gooley, P.R., Coffrey, M.S., Cusanovich, M.A. & MacKenzie, N.E. (1990) Assignment of the proton and nitrogen-15 NMR spectra of

Rhodobacter capsulatus ferrocytochrome c_2. *Biochemistry* **29**, 2278–2290.

10. Gooley, P.R., Coffrey, M.S., Cusanovich, M.A. & MacKenzie, N.E. (1992) Mutations Pro→Ala-35 and Tyr→Phe-75 of *Rhodobacter capsulatus* ferrocytochrome c_2 affects protein backbone dynamics: measurements of individual amide proton exchange rate constants by ^1H-^{15}N HMQC spectroscopy. *Biochemistry* **31**, 443–450.

11. Ehrhardt, M.R., Urbauer, J.L. & Wand, A.J. (1995) The energetics and dynamics of molecular recognition by calmodulin. *Biochemistry* **34**, 2731–2738.

12. Zhou, H.X., Hull, L.A., Kallenbach, N.R., Mayne, L., Bai, Y. & Englander, S.W. (1994) Quantitative evaluation of stabilizing interactions in a prenucleated α-helix by hydrogen exchange. *J. Am. Chem. Soc.* **116**, 6482–6483.

13. Andrec, M., Hill, R.B. & Prestegard, J.H. (1995) Amide exchange rates in *Escherichia coli* acyl carrier protein: Correlation with protein structure and dynamics. *Protein Sci.* **4**, 983–993.

14. Forsén, S. & Hoffman, R.A. (1963) Study of moderately rapid chemical exchange reactions by means of nuclear magnetic double resonance. *J. Chem. Phys.* **39**, 2892–2901.

15. Frenkiel, T.A. (1993) *NMR of Macromolecules. A Practical Approach* (Roberts, G.C.K., ed.) pp. 35–70, Oxford University Press, Oxford.

16. Bloembergen, N. & Pound, R.V. (1954) Radiation damping in magnetic resonance experiments. *Phys. Rev.* **95**, 8–12.

17. Altieri, A.S., Miller, K.E. & Byrd, R.A. (1996) A comparison of water suppression techniques using pulsed field gradients for high-resolution NMR of biomolecules. *Magn. Reson. Rev.* **17**, 27–82.

18. McConnell, H.M. (1958) Reaction rates by nuclear magnetic resonace. *J. Chem. Phys.* **28**, 430–431.

19. Ejchart, A., Siedlecka, M., Sticht, H. & Bierzyński, A. (1998) NMR studies of secondary structure in calcium binding hexadecapeptide. *Bull. Pol. Ac.: Chem.* **46**, 1–8.

20. Spera, S., Ikura, M. & Bax, A. (1991) Measurement of the exchange rates of rapidly exchanging amide protons: Application to the study of calmodulin and its complex with a myosin light chain kinase fragment. *J. Biomol. NMR* **1**, 155–165.

21. Peng, J.W. & Wagner, G. (1992) Mapping of the spectral densities of N–H bond motions in eglin *c* using heteronuclear relaxation experiments. *Biochemistry* **31**, 8571–8586.

22. Zangger, K. & Sterk, H. (1995) NMR studies of exchanging amide protons in 1-desamino-8-D-argininevasopressin by selective Hartmann-Hahn transfer. *Magn. Reson. Chem.* **33**, 124–127.

23. Redfield, A.G. & Waelder, S. (1979) Water solvent exchange rates of primary amides. Acid-catalyzed NMR saturation transfer as an indicator of rotation and structure of the protonated form. *J. Am. Chem. Soc.* **101**, 6151–6162.

24. Rosevear, P.R., Fry, D.C. & Mildvan, A.S. (1985) Temperature dependence of the longitudinal relaxation rates and exchange rates of the amide protons in peptide substrates of protein kinase. *J. Magn. Reson.* **61**, 102–115.

25. Henry, G.D. & Sykes, B.D. (1993) Saturation transfer of exchangeable protons in ^1H-decoupled ^{15}N INEPT spectra in water. Application to the measurement of hydrogen exchange rates in amides and proteins. *J. Magn. Reson.* **B102**, 193–200.

26. Adams, B. & Lerner, L. (1992) A simple one-dimensional method for measuring proton exchange rates in water. *J. Magn. Reson.* **96**, 604–607.

27. Böckmann, A. & Guittet, E. (1996) Suppression of radiation damping during selective ex-

citation of the water signal: The WANTED sequence. *J. Biomol. NMR* **8**, 87-92.

28. Morris, G.A. & Freeman, R. (1978) Selective excitation in Fourier transform nuclear magnetic resonance. *J. Magn. Reson.* **29**, 433-462.

29. Jeener, J., Meier, B.H., Bachman, P. & Ernst, R.R. (1979) Investigation of exchange processes by two-dimensional NMR spectroscopy. *J. Chem. Phys.* **71**, 4546-4553.

30. Schwartz, A.L. & Cutnell, J.D. (1983) One- and two-dimensional NMR studies of exchanging amide protons in glutathione. *J. Magn. Reson.* **53**, 398-411.

31. Maudsley, A.A. & Ernst, R.R. (1977) Indirect detection of magnetic resonance by heteronuclear two-dimensional spectroscopy. *Chem. Phys. Lett.* **50**, 368-372.

32. Bax, A., Griffey, R.H. & Hawkins, B.L. (1983) Correlation of proton and nitrogen-15 chemical shifts by multiple quantum NMR. *J. Magn. Reson.* **55**, 301-315.

33. Bodenhausen, G. & Reuben, D.J. (1980) Natural abundance nitrogen-15 NMR by enhanced heteronuclear spectroscopy. *Chem. Phys. Lett.* **69**, 185-189.

34. Hore, P.J. (1989) Solvent suppression. *Methods Enzymol.* **176**, 64-77.

35. Plateau, P. & Guéron, M. (1982) Exchangeable proton NMR without base-line distorsion, using new strong-pulse sequences. *J. Am. Chem. Soc.* **104**, 7310-7311.

36. Piotto, M., Saudek, V. & Sklenar, V. (1992) Gradient-tailored excitation for single-quantum NMR spectroscopy of aqueous solutions. *J. Biomol. NMR* **2**, 661-665.

37. Ejchart, A. (1998) Application of field gradients in high resolution NMR. *Bull. Pol. Ac.: Chem.* **46**, 117-131.

38. Abragam, A. (1989) *Principles of Nuclear Magnetism.* Chapter 8, Clarendon Press, Oxford.

39. Noggle, J.H. & Schirmer, R.E. (1971) *The Nuclear Overhauser Effect. Chemical Applications* Academic Press, New York, London.

40. Neuhaus, D. & Williamson, M.P. (1989) *The Nuclear Overhauser Effect in Structural and Conformational Analysis.* VCH Publishers, New York.

41. Campbell, I.D., Dobson, C.M. & Ratcliffe, R.G. (1977) Fourier transform proton NMR in H_2O. A method for measuring exchange and relaxation rates. *J. Magn. Reson.* **27**, 455-463.

42. Campbell, I.D., Dobson, C.M., Ratcliffe, R.G. & Williams, R.J.P. (1978) Fourier transform NMR pulse methods for the measurements of slow-exchange rates. *J. Magn. Reson.* **29**, 397-417.

43. Kriwacki, R.W., Hill, R.B., Flanagan, J.M., Caradonna, J.P. & Prestegard, J.H. (1993) New NMR methods for the characterization of bound waters in macromolecules. *J. Am. Chem. Soc.* **115**, 8907-8911.

44. Gemmecker, G., Jahnke, W. & Kessler, H. (1993) Measurement of fast proton exchange rates in isotopically labeled compounds. *J. Am. Chem. Soc.* **115**, 11620-11621.

45. Goch, G., Kozłowska, H., Wójtowicz, A. & Bierzyński, A. (1999) *Acta Biochim. Polon.* **46**, 673-678.

46. Freeman, R. & Hill, H.D.W. (1971) Fourier transform study of NMR spin-lattice relaxation by "progressive saturation". *J. Chem. Phys.* **54**, 3367-3377.

47. Zhukov, I. & Ejchart, A. (1999) Factors improving the accuracy of determination of ^{15}N relaxation parameters in proteins. *Acta Biochim. Polon.* **46**, 665-672.